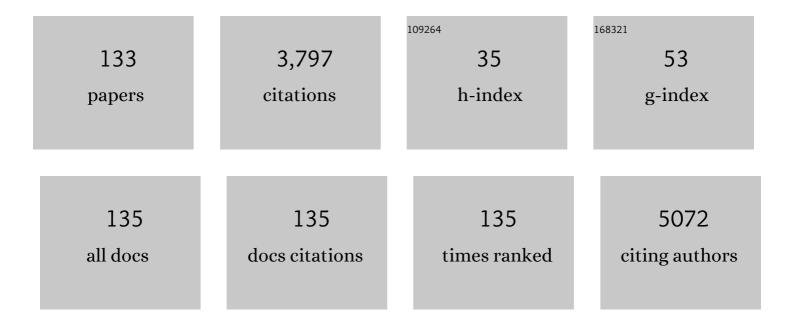
Piero Riello

List of Publications by Year in descending order

Source: https://exaly.com/author-pdf/5309088/publications.pdf Version: 2024-02-01



D

#	Article	IF	CITATIONS
1	Synthesis of magnetic nanoparticles by laser ablation of strontium ferrite under water and their characterization by optically detected magnetophoresis supported by BEM calculations. Journal of Materials Chemistry C, 2022, 10, 3819-3825.	2.7	4
2	Mesoporous zirconia nanoparticles as drug delivery systems: Drug loading, stability and release. Journal of Drug Delivery Science and Technology, 2021, 61, 102189.	1.4	7
3	Ag-sensitized Tb3+/Yb3+ codoped silica-zirconia glasses and glass-ceramics: Systematic and detailed investigation of the broadband energy-transfer and downconversion processes. Ceramics International, 2021, 47, 17939-17949.	2.3	9
4	Confined-Melting-Assisted Synthesis of Bismuth Silicate Glass-Ceramic Nanoparticles: Formation and Optical Thermometry Investigation. ACS Applied Materials & Interfaces, 2020, 12, 55195-55204.	4.0	35
5	Upconversion-mediated Boltzmann thermometry in double-layered Bi ₂ SiO ₅ :Yb ³⁺ ,Tm ³⁺ @SiO ₂ hollow nanoparticles. Journal of Materials Chemistry C, 2020, 8, 7828-7836.	2.7	61
6	Ag-Sensitized NIR-Emitting Yb3+-Doped Glass-Ceramics. Applied Sciences (Switzerland), 2020, 10, 2184.	1.3	10
7	Lanthanide-Doped Bi ₂ SiO ₅ @SiO ₂ Core–Shell Upconverting Nanoparticles for Stable Ratiometric Optical Thermometry. ACS Applied Nano Materials, 2020, 3, 2594-2604.	2.4	55
8	Zirconia-Based Magnetoplasmonic Nanocomposites: A New Nanotool for Magnetic-Guided Separations with SERS Identification. ACS Applied Nano Materials, 2020, 3, 1232-1241.	2.4	14
9	Large-Scale CMOS-Compatible Process for growing Si-BC8 Nanowires. , 2020, , .		0
10	Lanthanide-Doped Bismuth-Based Fluoride Nanocrystalline Particles: Formation, Spectroscopic Investigation, and Chemical Stability. Chemistry of Materials, 2019, 31, 8504-8514.	3.2	29
11	Bi ₂ SiO ₅ @g-SiO ₂ upconverting nanoparticles: a bismuth-driven core–shell self-assembly mechanism. Nanoscale, 2019, 11, 675-687.	2.8	31
12	Growth of nanostructured silicon by microwave/nano-susceptors technique with low substrate temperature. Materials Science in Semiconductor Processing, 2019, 100, 22-28.	1.9	1
13	Silicon nanowires to detect electric signals from living cells. Materials Research Express, 2019, 6, 084005.	0.8	9
14	Bismuth titanate-based UV filters embedded mesoporous silica nanoparticles: Role of bismuth concentration in the self-sealing process. Journal of Colloid and Interface Science, 2019, 549, 1-8.	5.0	24
15	High-temperature compressive creep of novel fine-grained orthorhombic ZrO 2 ceramics stabilized with 12†mol% Ta doping. Journal of the European Ceramic Society, 2018, 38, 2445-2448.	2.8	5
16	Insight into the Upconversion Luminescence of Highly Efficient Lanthanide-Doped Bi ₂ O ₃ Nanoparticles. Journal of Physical Chemistry C, 2018, 122, 7389-7398.	1.5	28
17	Some crystallographic considerations on the novel orthorhombic ZrO 2 stabilized with Ta doping. Ceramics International, 2018, 44, 10362-10366.	2.3	6
18	CMOS Compatible, Low Temperature, growth of Silicon Nanowires by Microwave nano-susceptors. , 2018, , .		1

#	Article	IF	CITATIONS
19	Inorganic Nanoparticles for Cancer Therapy: A Transition from Lab to Clinic. Current Medicinal Chemistry, 2018, 25, 4269-4303.	1.2	150
20	Ag-Sensitized Yb3+ Emission in Glass-Ceramics. Micromachines, 2018, 9, 380.	1.4	10
21	Ag nanoaggregates as efficient broadband sensitizers for Tb3+ ions in silica-zirconia ion-exchanged sol-gel glasses and glass-ceramics. Optical Materials, 2018, 84, 668-674.	1.7	14
22	Carbon Dots from Sugars and Ascorbic Acid: Role of the Precursors on Morphology, Properties, Toxicity, and Drug Uptake. ACS Medicinal Chemistry Letters, 2018, 9, 832-837.	1.3	95
23	Role of Ag multimers as broadband sensitizers in Tb3+/Yb3+ co-doped glass-ceramics. , 2018, , .		1
24	Continuousâ€Flow <i>O</i> â€Alkylation of Biobased Derivatives with Dialkyl Carbonates in the Presence of Magnesium–Aluminium Hydrotalcites as Catalyst Precursors. ChemSusChem, 2017, 10, 1571-1583.	3.6	13
25	Bottom-up synthesis of carbon nanoparticles with higher doxorubicin efficacy. Journal of Controlled Release, 2017, 248, 144-152.	4.8	51
26	Tuning the upconversion light emission by bandgap engineering in bismuth oxide-based upconverting nanoparticles. Nanoscale, 2017, 9, 6353-6361.	2.8	33
27	Orthorhombic phase stabilization and transformation phase process in zirconia tantalum-doped powders and spark plasma sintering systems. Journal of the European Ceramic Society, 2017, 37, 3393-3401.	2.8	6
28	Ceramics of Ta-doping stabilized orthorhombic ZrO2 densified by spark plasma sintering and the effect of post-annealing in air. Scripta Materialia, 2017, 130, 128-132.	2.6	14
29	Formation and Controlled Growth of Bismuth Titanate Phases into Mesoporous Silica Nanoparticles: An Efficient Self-Sealing Nanosystem for UV Filtering in Cosmetic Formulation. ACS Applied Materials & Interfaces, 2017, 9, 1913-1921.	4.0	53
30	Pegylated silica nanoparticles: cytotoxicity and macrophage uptake. Journal of Nanoparticle Research, 2017, 19, 1.	0.8	11
31	Towards life in hydrocarbons: aggregation behaviour of "reverse―surfactants in cyclohexane. RSC Advances, 2017, 7, 15337-15341.	1.7	10
32	Towards a Rational Design of a Continuous-Flow Method for the Acetalization of Crude Glycerol: Scope and Limitations of Commercial Amberlyst 36 and AlF3·3H2O as Model Catalysts. Molecules, 2016, 21, 657.	1.7	27
33	Small-angle scattering behavior of thread-like and film-like systems. Journal of Applied Crystallography, 2016, 49, 260-276.	1.9	3
34	On the synthesis and thermal stability of RuN, an uncommon nitride. Surface and Coatings Technology, 2016, 295, 93-98.	2.2	6
35	Determining europium compositional fluctuations in partially stabilized zirconia nanopowders: a non-line-broadening-based method. Acta Crystallographica Section B: Structural Science, Crystal Engineering and Materials, 2016, 72, 29-38.	0.5	3
36	3-D flower like Ce–Zr–Cu mixed oxide systems in the CO preferential oxidation (CO-PROX): Effect of catalyst composition. Applied Catalysis B: Environmental, 2015, 168-169, 385-395.	10.8	55

#	Article	IF	CITATIONS
37	Phosphonium-based tetrakis dibenzoylmethane Eu(<scp>iii</scp>) and Sm(<scp>iii</scp>) complexes: synthesis, crystal structure and photoluminescence properties in a weakly coordinating phosphonium ionic liquid. RSC Advances, 2015, 5, 60898-60907.	1.7	22
38	Biocompatible tailored zirconia mesoporous nanoparticles with high surface area for theranostic applications. Journal of Materials Chemistry B, 2015, 3, 7300-7306.	2.9	25
39	Laser generation of iron-doped silver nanotruffles with magnetic and plasmonic properties. Nano Research, 2015, 8, 4007-4023.	5.8	61
40	On the synthesis of a compound with positive enthalpy of formation: Zinc-blende-like RuN thin films obtained by rf-magnetron sputtering. Applied Surface Science, 2014, 320, 863-870.	3.1	11
41	Structural and photophysical properties of rare-earth complexes encapsulated into surface modified mesoporous silica nanoparticles. Dalton Transactions, 2014, 43, 16183-16196.	1.6	27
42	Energy Transfer in Bi- and Er-Codoped Y ₂ O ₃ Nanocrystals: An Effective System for Rare Earth Fluorescence Enhancement. Journal of Physical Chemistry C, 2014, 118, 30071-30078.	1.5	43
43	Mesoporous silica nanoparticles with tunable pore size for tailored gold nanoparticles. Journal of Nanoparticle Research, 2014, 16, 1.	0.8	29
44	TiO ₂ –mesoporous silica nanocomposites: cooperative effect in the photocatalytic degradation of dyes and drugs. RSC Advances, 2014, 4, 37826-37837.	1.7	47
45	Oxygen Hole States in Zirconia Lattices: Quantitative Aspects of Their Cathodoluminescence Emission. Journal of Physical Chemistry A, 2014, 118, 9828-9836.	1.1	26
46	Energy transfer between Tb3+ and Eu3+ in co-doped Y2O3 nanocrystals prepared by Pechini method. Journal of Nanoparticle Research, 2013, 15, 1.	0.8	36
47	Monitoring the <i>t → m</i> Martensitic Phase Transformation by Photoluminescence Emission in <scp><scp>Eu</scp></scp> ³⁺ â€Doped Zirconia Powders. Journal of the American Ceramic Society, 2013, 96, 2628-2635.	1.9	40
48	Unexpected optical activity of cerium in Y ₂ O ₃ :Ce ³⁺ , Yb ³⁺ , Er ³⁺ up and down-conversion system. Dalton Transactions, 2013, 42, 16837-16845.	1.6	25
49	Er and Cu codoped SiO2 films obtained by sputtering deposition: Enhancement of the rare earth emission at 1.541¼m mediated by metal sensitizers. Optical Materials, 2013, 35, 2018-2022.	1.7	15
50	pH-activated doxorubicin release from polyelectrolyte complex layer coated mesoporous silica nanoparticles. Microporous and Mesoporous Materials, 2013, 180, 86-91.	2.2	36
51	<i>In situ</i> reaction furnace for real-time XRD studies. Journal of Synchrotron Radiation, 2013, 20, 194-196.	1.0	33
52	Combustion synthesis and photoluminescence of Tb3+ doped LaAlO3 nanophosphors. Optical Materials, 2013, 35, 1184-1188.	1.7	27
53	Coexistence of plasmonic and magnetic properties in Au89Fe11 nanoalloys. Nanoscale, 2013, 5, 5611.	2.8	92
54	In situ synthesis of Eu(Tp)3 complex inside the pores of mesoporous silica nanoparticles. Journal of Luminescence, 2013, 142, 28-34.	1.5	9

#	Article	IF	CITATIONS
55	Influence of synthesis parameters on the performance of CeO2–CuO and CeO2–ZrO2–CuO systems in the catalytic oxidation of CO in excess of hydrogen. Applied Catalysis B: Environmental, 2013, 129, 556-565.	10.8	67
56	Structural and magnetic properties of mesoporous SiO2 nanoparticles impregnated with iron oxide or cobalt-iron oxide nanocrystals. Journal of Materials Chemistry, 2012, 22, 19276.	6.7	35
57	Optical investigation of Tb3+-doped Y2O3 nanocrystals prepared by Pechini-type sol–gel process. Journal of Nanoparticle Research, 2012, 14, 1.	0.8	42
58	Photoluminescence properties of YAG:Ce3+,Pr3+ phosphors synthesized via the Pechini method for white LEDs. Journal of Nanoparticle Research, 2012, 14, 1.	0.8	40
59	Sol–gel preparation and characterization of nano-crystalline lithium–mica glass–ceramic. Ceramics International, 2012, 38, 2813-2821.	2.3	18
60	Preparation, characterization and single-cell performance of a new class of Pd-carbon nitride electrocatalysts for oxygen reduction reaction in PEMFCs. Applied Catalysis B: Environmental, 2012, 111-112, 185-199.	10.8	56
61	Self-assembly in surfactant-based liquid mixtures: Octanoic acid/Bis(2-ethylhexyl)amine systems. Journal of Colloid and Interface Science, 2012, 367, 280-285.	5.0	35
62	Nucleation and crystallization behaviors of nano-crystalline lithium–mica glass–ceramic prepared via sol–gel method. Materials Research Bulletin, 2012, 47, 1374-1378.	2.7	7
63	Top-down synthesis of multifunctional iron oxide nanoparticles for macrophage labelling and manipulation. Journal of Materials Chemistry, 2011, 21, 3803.	6.7	82
64	Magnetic Nanoparticles of Iron Carbide, Iron Oxide, Iron@Iron Oxide, and Metal Iron Synthesized by Laser Ablation in Organic Solvents. Journal of Physical Chemistry C, 2011, 115, 5140-5146.	1.5	204
65	Magnetic iron oxide nanoparticles with tunable size and free surface obtained via a "green―approach based on laser irradiation in water. Journal of Materials Chemistry, 2011, 21, 18665.	6.7	55
66	Synthesis and optical properties of sub-micron sized rare earth-doped zirconia particles. Optical Materials, 2011, 33, 1745-1752.	1.7	46
67	Effect of thermal treatments on the catalytic behaviour in the CO preferential oxidation of a CuO–CeO2–ZrO2 catalyst with a flower-like morphology. Applied Catalysis B: Environmental, 2011, 102, 627-637.	10.8	98
68	Er-doped alumina crystalline films deposited by radiofrequency magnetron co-sputtering. Optical Materials, 2011, 33, 1135-1138.	1.7	13
69	Structural and luminescence properties of europium(III)-doped zirconium carbonates and silica-supported Eu3+-doped zirconium carbonate nanoparticles. Journal of Nanoparticle Research, 2010, 12, 993-1002.	0.8	15
70	Comparison of Eu(NO3)3 and Eu(acac)3 precursors for doping luminescent silica nanoparticles. Journal of Nanoparticle Research, 2010, 12, 1925-1931.	0.8	23
71	Renewable H ₂ from Glycerol Steam Reforming: Effect of La ₂ O ₃ and CeO ₂ Addition to Pt/Al ₂ O ₃ catalysts ChemSusChem, 2010, 3, 619-628.	3.6	53
72	Structural and photoluminescence properties of ZrO2:Eu3+ @ SiO2 nanophosphors as a function of annealing temperature. Journal of Luminescence, 2010, 130, 2429-2436.	1.5	28

#	Article	IF	CITATIONS
73	Investigation of luminescent dye-doped or rare-earth-doped monodisperse silica nanospheres for DNA microarray labelling. Optical Materials, 2010, 32, 1652-1658.	1.7	22
74	Er-doped dielectric films by radiofrequency magnetron co-sputtering. Surface and Coatings Technology, 2010, 204, 2023-2027.	2.2	3
75	A multinuclear solid-state magnetic resonance study on submicrometer-sized SiO2 particles encapsulated by a PMMA shell. Colloids and Surfaces A: Physicochemical and Engineering Aspects, 2010, 369, 191-195.	2.3	3
76	Evolution of the Nonionic Inverse Microemulsionâ^'Acidâ^'TEOS System during the Synthesis of Nanosized Silica via the Solâ^'Gel Process. Langmuir, 2010, 26, 12917-12925.	1.6	18
77	Encapsulation of submicrometer-sized silica particles by a thin shell of poly(methyl methacrylate). Journal of Colloid and Interface Science, 2009, 331, 351-355.	5.0	37
78	X-ray powder diffraction quantitative analysis of an amorphous SiO2–poly(methyl methacrylate) nanocomposite. Journal of Applied Crystallography, 2008, 41, 985-990.	1.9	4
79	Effect of the synthetic parameters on the textural properties of one-pot mesoporous Al–Ce–Cu systems. Microporous and Mesoporous Materials, 2008, 116, 575-580.	2.2	11
80	Synthesis and characterization of monodisperse Eu-doped luminescent silica nanospheres for biological applications. , 2008, , .		8
81	Time-Resolved in Situ Small-Angle X-ray Scattering Study of Silica Particle Formation in Nonionic Water-in-Oil Microemulsions. Langmuir, 2008, 24, 5225-5228.	1.6	21
82	Solid acid catalysts from clays: Preparation of mesoporous catalysts by chemical activation of metakaolin under acid conditions. Journal of Colloid and Interface Science, 2007, 311, 537-543.	5.0	80
83	Small-angle scattering from three-phase samples: application to coal undergoing an extraction process. Journal of Applied Crystallography, 2007, 40, 282-289.	1.9	14
84	Enhanced low-temperature protonic conductivity in fully dense nanometric cubic zirconia. Applied Physics Letters, 2006, 89, 163116.	1.5	45
85	Effect of the microstructure on concentration quenching in heavily doped Tb2O3–ZrO2 nanoparticles embedded in silica. Chemical Physics Letters, 2006, 431, 326-331.	1.2	11
86	Erbium-doped LAS glass ceramics prepared by spark plasma sintering (SPS). Journal of the European Ceramic Society, 2006, 26, 3301-3306.	2.8	29
87	Reduction of concentration-induced luminescence quenching in Eu3+-doped nanoparticles embedded in silica. Optical Materials, 2006, 28, 1261-1265.	1.7	18
88	Nanoscale Effects on the Ionic Conductivity of Highly Doped Bulk Nanometric Cerium Oxide. Advanced Functional Materials, 2006, 16, 2363-2368.	7.8	79
89	Synthesis, X-ray Diffraction Characterization, and Radiative Properties of Er2O3â^'ZrO2Nanocrystals Embedded in LAS Glass Ceramic. Journal of Physical Chemistry B, 2005, 109, 13424-13430.	1.2	13
90	Preparation, structural characterization, and luminescence properties of Eu3+-doped nanocrystalline ZrO2. Journal of Materials Research, 2005, 20, 2780-2791.	1.2	59

#	Article	IF	CITATIONS
91	Synthesis and luminescence properties of ZrO2 and ZrO2/SiO2 composites incorporating Eu(III)–phenanthroline complex prepared by a catalyst-free sol–gel process. Optical Materials, 2004, 27, 249-255.	1.7	13
92	AFM, SEM and GIXRD studies of thin films of red polycarbazolyldiacetylenes. Surface Science, 2004, 554, 68-75.	0.8	6
93	A comparative study of primary Al precipitation in amorphous Al87Ni7La5Zr by means of WAXS, SAXS, TEM and DSC techniques. Acta Materialia, 2004, 52, 5031-5041.	3.8	24
94	Radiofrequency magnetron co-sputtering deposition synthesis of Co-based nanocomposite glasses for optical and magnetic applications. Applied Surface Science, 2004, 226, 62-67.	3.1	10
95	Quantitative Analysis of Amorphous Fraction in the Study of the Microstructure of Semi-crystalline Materials. Springer Series in Materials Science, 2004, , 167-184.	0.4	15
96	Structure and Size of Poly-Domain Pd Nanoparticles Supported on Silica. Catalysis Letters, 2003, 88, 141-146.	1.4	26
97	Wustite as a new precursor of industrial ammonia synthesis catalysts. Applied Catalysis A: General, 2003, 251, 121-129.	2.2	53
98	Synchrotron SAXS Study of the Mechanisms of Aggregation of Sulfate Zirconia Sols. Journal of Physical Chemistry B, 2003, 107, 3390-3399.	1.2	22
99	Quantitative investigations of supported metal catalysts by ASAXS. Journal of Synchrotron Radiation, 2002, 9, 65-70.	1.0	22
100	Thermal Evolution of Carbon-Supported Pd Nanoparticles Studied by Time-Resolved X-ray Diffraction. Journal of Physical Chemistry B, 2001, 105, 8088-8091.	1.2	22
101	Nucleation and crystallization behavior of glass-ceramic materials in the Li2O–Al2O3–SiO2 system of interest for their transparency properties. Journal of Non-Crystalline Solids, 2001, 288, 127-139.	1.5	106
102	Nanostructure of Pd/SiO2 supported catalysts. Physical Chemistry Chemical Physics, 2001, 3, 4614-4619.	1.3	21
103	Small angle scattering of Ag–1 wt.% Mg alloys internally oxidized at high temperatures: a model of interacting spherical clusters. Physical Chemistry Chemical Physics, 2001, 3, 3213-3216.	1.3	3
104	Alumina-Promoted Sulfated Zirconia System:Â Structure and Microstructure Characterization. Chemistry of Materials, 2001, 13, 1634-1641.	3.2	57
105	Detecting palladium nanoparticles in Pd/C catalysts using Xâ€ray Rietveld method. Catalysis Letters, 2000, 64, 119-124.	1.4	13
106	In situ wide angle X-ray scattering (WAXS) study of bimetallic Au–Pd catalysts. Catalysis Letters, 2000, 69, 17-20.	1.4	6
107	Low-loaded metal Pd-Au supported catalysts on active carbon. Recent developments of the X-ray diffraction analysis to detect simultaneously nanoclusters and larger particles. Studies in Surface Science and Catalysis, 2000, , 3273-3278.	1.5	2
108	Nanostructural Features of Pd/C Catalysts Investigated by Physical Methods:Â A Reference for Chemisorption Analysis. Langmuir, 2000, 16, 4539-4546.	1.6	63

#	Article	IF	CITATIONS
109	Stabilization of cubic Na-modified ZrO2: a neutron diffraction study. Journal of Applied Crystallography, 1999, 32, 475-480.	1.9	11
110	ASAXS study of Au, Pd and Pd–Au catalysts supported on active carbon. Catalysis Today, 1999, 49, 485-489.	2.2	35
111	Small-angle X-ray scattering and Rayleigh scattering studies of the microstructure of some optical glasses. Journal of Non-Crystalline Solids, 1999, 258, 198-206.	1.5	2
112	Quantitative Phase Analysis in Semicrystalline Materials Using the Rietveld Method. Journal of Applied Crystallography, 1998, 31, 78-82.	1.9	52
113	Scale Factor in Powder Diffraction. Acta Crystallographica Section A: Foundations and Advances, 1998, 54, 219-224.	0.3	13
114	The microstructure of borosilicate glasses containing elongated and oriented phase-separated crystalline particles. Journal of Non-Crystalline Solids, 1998, 232-234, 147-154.	1.5	7
115	Au/C Catalyst:  Experimental Evidence of the Coexistence of Nanoclusters and Larger Au Particles. Langmuir, 1998, 14, 6617-6619.	1.6	27
116	Calibration of the monochromator bandpass function for the X-ray Rietveld analysis. Powder Diffraction, 1997, 12, 160-166.	0.4	24
117	Small angle scattering of a polydisperse system of interacting hard spheres: An analytical solution. Journal of Chemical Physics, 1997, 106, 8660-8663.	1.2	16
118	ASAXS Investigation of a Au/C Catalyst. Journal of Catalysis, 1997, 171, 345-348.	3.1	23
119	Two-Dimensional Small-Angle X-ray Scattering Investigation of Stretched Borosilicate Glasses. Journal of Applied Crystallography, 1997, 30, 487-494.	1.9	6
120	Two-dimensional small-angle X-ray scattering investigation of stretched borosilicate glasses. Erratum. Journal of Applied Crystallography, 1997, 30, 1159-1159.	1.9	0
121	Redrawn Phase-Separated Borosilicate Glasses: A TEM Investigation. Microscopy Microanalysis Microstructures, 1997, 8, 157-165.	0.4	5
122	A semi-empirical asymmetry function for X-ray diffraction peak profiles. Powder Diffraction, 1995, 10, 204-206.	0.4	9
123	X-ray Rietveld Analysis with a Physically Based Background. Journal of Applied Crystallography, 1995, 28, 115-120.	1.9	43
124	Determining the Degree of Crystallinity in Semicrystalline Materials by means of the Rietveld Analysis. Journal of Applied Crystallography, 1995, 28, 121-126.	1.9	22
125	Fractal model of amorphous and semicrystalline nano-sized zirconia aerogels. Journal of Non-Crystalline Solids, 1995, 185, 78-83.	1.5	20
126	Physicochemical properties of thermally prepared Ti-supported IrO2+ ZrO2 electrocatalysts. Journal of Electroanalytical Chemistry, 1994, 376, 195-202.	1.9	39

#	Article	IF	CITATIONS
127	SAXS study of the micro-inhomogeneity of industrial soda lime silica glass. Journal of Non-Crystalline Solids, 1994, 167, 263-271.	1.5	4
128	Short-range structure of zirconia xerogel and aerogel, determined by wide angle X-ray scattering. Journal of Non-Crystalline Solids, 1993, 155, 259-266.	1.5	11
129	Fractal properties of a partially crystalline zirconium oxide aerogel. Journal of Applied Crystallography, 1993, 26, 717-720.	1.9	19
130	Complete sets of factors for absorption correction and air scattering subtraction in X-ray powder diffraction of loosely packed samples. Powder Diffraction, 1993, 8, 149-154.	0.4	14
131	Structural characterization of Cd(Se, S)-doped glasses. Journal of Non-Crystalline Solids, 1992, 142, 63-69.	1.5	7
132	XRD investigation of the crystallization process in Fe40Ni40B20 metallic glass. Journal of Non-Crystalline Solids, 1992, 151, 59-65.	1.5	3
133	X-Ray diffraction characterization of iridium dioxide electrocatalysts. Journal of Materials Chemistry, 1991, 1, 511.	6.7	21